Published in final edited form as:
J Magn Reson Imaging. 2011 October ; 34(4): 968–972. doi:10.1002/jmri.22667.

Windowed Stochastic Proton Decoupling for in Vivo ^{13}C Magnetic Resonance Spectroscopy with Reduced RF Power Deposition

Yun Xiang, MD, PhD and **Jun Shen, PhD**[*]
Molecular Imaging Branch, National Institute of Mental Health Intramural Research Program, National Institutes of Health, Bethesda, MD, United States

Abstract

Purpose—To propose a strategy for reducing RF power deposition by stochastic proton decoupling based on Rayleigh's theorem.

Materials and Methods—Rayleigh's theorem was used to remove frequency components of stochastic decoupling over the 3.90–6.83 ppm range. [2-^{13}C] or [2,5-$^{13}C_2$]glucose was infused intravenously to anesthetized rats. ^{13}C labeling of brain metabolites was detected in the carboxylic/amide spectral region at 11.7 Tesla using either the original stochastic decoupling method developed by Ernst or the proposed windowed stochastic decoupling method.

Results—By restricting frequency components of stochastic decoupling to 1.91–3.90 ppm and 6.83–7.60 ppm spectral regions decoupling power deposition was reduced by ~50%. The proposed windowed stochastic decoupling scheme is experimentally demonstrated for in vivo ^{13}C MRS of rat brain at 11.7 Tesla.

Conclusion—The large reduction in decoupling power deposition makes it feasible to perform stochastic proton decoupling at very high magnetic fields for human brain ^{13}C MRS studies.

Keywords

In vivo ^{13}C MRS; carboxylic/amide carbons; stochastic decoupling scheme; RF power deposition

Proton decoupled in vivo ^{13}C magnetic resonance specetrscopy (MRS) is a useful noninvasive method for studying animal and human brain metabolism and neurotransmitter cycling. With the enhanced ^{13}C signal due to infusion of exogenous ^{13}C-labeled substrates such as glucose, the turnover of important metabolites in brain can be quantitatively measured (1–8). One of the major difficulties associated with ^{13}C MRS has been the need to decouple large ^{1}H-^{13}C scalar couplings ($^{1}J_{CH}$ = 125–145 Hz) for alkyl carbons of major brain metabolites. Tissue heating due to RF losses associated with electrically conducting samples places a restriction on RF power deposition. For effective proton decoupling, the radio frequency field strength of decoupling pulses (γB_2) has to be much greater than $^{1}J_{CH}$. Because chemical shift dispersion is proportional to static magnetic field strength (γB_0), the proton decoupling bandwidth andγB_2 increase linearly with γB_0. Therefore, RF power required for proton decoupling increases as a function of $(\gamma B_0)^2$, a formidable challenge for performing ^{13}C MRS at high magnetic field strength. To obtain necessary RF efficiency with acceptable RF power deposition, most human brain ^{13}C MRS studies have used the coherent cyclic WALTZ sequence for proton decoupling at 1.5–4 Tesla (2–4, 8) at

[*]Address reprint requests to: J. S., Molecular Imaging Branch, National Institute of Mental Health, National Institutes of Health, Bldg. 10, Rm. 2D51A, 9000 Rockville Pike, Bethesda, MD 20892-1527. shenj@intra.nimh.nih.gov.

decoupling power levels just under the SAR threshold set by the FDA. Coherent cyclic decoupling sequences such as MLEV and WALTZ achieve broadband decoupling of protons so that the CH splittings are eliminated from ^{13}C spectra over the entire range of proton chemical shifts. As such, they have long superseded stochastic decoupling (9) in modern NMR spectroscopy. At very low γB_2, however, coherent decoupling schemes break down quickly (10) because a single cycle of WALTZ-4 may occupy a significant portion of the FID sampling time.

A new strategy for in vivo ^{13}C MRS was developed recently (10). Instead of infusing the commonly used [1-^{13}C]glucose which primarily labels the alkyl carbons of amino acids we infused [2-^{13}C] or [2,5-$^{13}C_2$]glucose and detected the ^{13}C signals of glutamate, glutamine, γ-aminobutyric acid (GABA), aspartate, and N-acetylaspartate (NAA) in the carboxylic/amide spectral region. The carboxylic/amide carbons are only coupled to protons via weak long-range ^{1}H-^{13}C couplings. It was found that these carbons could be effectively decoupled using stochastic decoupling schemes with very low RF power. In sharp contrast to the alkyl spectral region, no interfering lipid signals were found in the carboxylic/amide spectral region for brain studies.

Because decoupling power increases as a function of $(\gamma B_0)^2$ even stochastic decoupling may become problematic at very high magnetic field strength. For brain ^{13}C MRS studies using the carboxylic/amide spectral region, the protons to be decoupled are clustered in two specific regions of the spectrum: the alkyl protons resonating at 1.91 (GABA H3)-3.90 (aspartate H2) ppm and the amide protons resonating at 6.83 (Gln H_Z)-7.60 (Gln H_E) ppm. Using white or pseudo white stochastic decoupling schemes considerable RF power is wasted in the empty spectral window spanning the 3.90–6.83 ppm region because the spectral density function (i.e., the Fourier transform of the autocorrelation function δ) of ideal white noise is independent of frequency. We realize that a large reduction in RF power deposition (≈50%) for stochastic decoupling is achievable if the large empty spectral window could be excluded from the effective band of stochastic decoupling sequences.

In this work, we propose a strategy for reducing RF power deposition of stochastic proton decoupling. The proposed method is based on the Rayleigh's theorem (11), which states that the total power in a signal is invariant with respect to Fourier transform. That is, the power calculated in the time domain and the frequency domain is the same. Since proton spins are decoupled by frequency components at and near their resonance frequency we multiplied the frequency spectrum of the stochastic decoupling pulse by an ideal double bandpass filter with rectangular response functions that eliminates frequency components outside the 1.91–3.90 ppm and 6.83–7.60 ppm regions. The effect of the proposed method on the performance of the stochastic decoupling sequence was demonstrated experimentally for localized in vivo ^{13}C MRS of rat brain at 11.7 Tesla.

MATRIALS AND METHODS

Male Sprague-Dawley rats (Taconic, Germantown, NY, USA; 178–211 g, n = 3) fasted for 24 hrs with free access to drinking water were used to test the proposed stochastic decoupling sequences. The animal study protocol was approved by the National Institute of Mental Health Animal Care and Use Committee. The animals were orally intubated and ventilated with a mixture of 70% N_2O/30% O_2 and 1.5% isoflurane. The left femoral artery was cannulated where plasma samples were withdrawn periodically for monitoring blood physiology using a blood analyzer (Bayer Rapidlab 860, East Walpole, MA). The left femoral vein was cannulated for infusion of [2-^{13}C]glucose or [2,5-$^{13}C_2$]glucose (99% enrichment, Cambridge Isotope Labs, Andover, MA, 0.75 M) with an initial bolus at 113 mg/kg/min followed by infusion at a reduced rate (42.8 mg/kg/min) which was adjusted

over a small range to maintain constant plasma glucose level. The glucose infusion protocol rapidly raised plasma glucose concentration to and maintained it at 16.14 ± 2.16 mM. Rectal temperature was maintained at 37.5 ± 0.5°C using an external pump for water circulation (BayVoltex, Modesto, CA). Normal arterial blood physiological parameters were maintained by small adjustments of respiration rate and volume. End-tidal CO_2, tidal pressure of ventilation, and heart rate were also monitored. The initial ~1.5 hr glucose infusion period was used for another experiment not described in this report.

All experiments were performed on a Bruker AVANCE spectrometer (Bruker Biospin, Billerica, MA) interfaced to an 11.7 Tesla 89-mm bore vertical magnet (Magnex Scientific, Abingdon, UK) located in a room without RF shielding. The spectrometer is equipped with a 57-mm i.d. gradient (Mini 0.5, Bruker Biospin, Billerica, MA, with a maximum gradient strength of 3.0 G/mm and a rise time of 100 μs) for studying young adult rats in vivo. A home-built integrated RF surface coils/head holder system mounted on a half-cylindrical plastic cradle was used (12). The ^{13}C and ^{1}H RF coils were coplanar and made of single-sided printed circuit board. The inner loop of the RF assembly is the ^{13}C coil with an inner diameter and conductor width of 10.8 mm and 4.3 mm, respectively. The outer loop is the ^{1}H coil with an inner diameter and conductor width of 23.6 mm and 5.4 mm, respectively. To provide shielding against ambient RF noise, the main body of the RF probe/animal handling system was built using an aluminum tube with an outer diameter of 56.6 mm. The lower end of the integrated RF surface coils/head holder system was an aluminum interface box for connecting RF cables, ventilation tubes, fiber-optic rectal thermal probe, and catheters. The RF probe/animal handling system also provides rat head fixation and body support. It allows maintenance of normal physiology despite of increased cardiac load and blood draining associated with vertical positioning (12). The animal handling system was mechanically interfaced to the magnet using an adaptor ring which allows vertical and angular positional adjustments. Commercial broadband low-pass and high-pass filters (Bruker Biospin, Billerica, MA) were inserted before the preamplifiers.

Three-slice (coronal, horizontal, and sagittal) scout RARE images (FOV = 2.5 cm, slice thickness = 1 mm, TR/TE = 200/15 ms, rare factor = 8, 128 × 128 data matrix) were acquired first for positioning the RF probe/animal handling system inside the Bruker Mini 0.5 gradient insert. After positioning, the gradient isocenter was 0 – 1 mm posterior to bregma based on separate calibrations. An 8.5 × 6 × 8.5 mm^3 (434 μL) spectroscopy voxel was placed at the gradient isocenter along the brain midline. The rat brain was shimmed as described previously using the FLATNESS methods (13). A train of non-selective hard pulses with a nominal flip angle of 180° spaced at 100 ms apart was used for generation of broadband $^{1}H \rightarrow ^{13}C$ heteronuclear Overhauser enhancement. Direct three-dimensional spatial localization of ^{13}C spins in the carboxylic/amide region uses a 0.75 ms adiabatic half-passage pulse followed by three pairs of hyperbolic secant pulses (one pair per dimension, 2-ms per pulse with phase factor = 5 and truncation level = 1%) as described previously (14). The ^{13}C 180° pulses also refocus the long-range heteronuclear ^{1}H-^{13}C couplings during TE. No additional outer volume suppression schemes were found necessary. TR/TE = 20000/18 ms. Spectral width was set to 10 kHz with a sampling time of 204.8 ms. The stochastic decoupling waveforms were generated using a random noise generation routine in MATLAB, which creates a sequence of random numbers with an equal probability of occurrence over a predefined range. During the data sampling time, ^{1}H decoupling was applied which uses the pseudo noise decoupling schemes described by Ernst (constant γB_2 amplitude, randomly inverted phases (9), and a repetition unit of 0.35 ms) and the proposed reduced power stochastic decoupling scheme. For each data block 30 scans were acquired. Prior to Fourier transform, the time-domain data were zero-padded to 16 K. gb = 0.06, lb = −1. The ^{13}C signals in the carboxylic/amide region were analyzed using Bruker Biospin XWINNMR software (Bruker Biospin, Billerica, MA). The ^{13}C carrier

frequency was placed around 180.4 ppm. The proton decoupler frequency was placed at 4.82 ppm.

RESULTS

For the application described here, the original pseudo noise sequence proposed by Ernst was produced with the phase of each segment randomly chosen to be either 0° or 180° (Fig 1(a, b)). A total of 585 segments were used to span the data sampling time of 204.8 ms. Then this pseudo noise sequence is Fourier transformed (Fig. 1(c, d)). Note that the frequency response is linearly scalable by changing the duration of the segments. To avoid forwarding RF power to the 3.90–6.83 ppm region, according to Rayleigh's theorem, the corresponding frequency components should be removed. This was achieved by multiplying the both the real and imaginary frequency response of the original pseudo noise decoupling sequence by an ideal double bandpass filter as depicted in Fig. 2(a, b). The two bands correspond to the 1.91–3.90 ppm and 6.83–7.60 ppm regions with a margin of 0.1 ppm on both sides of each band to offset B_0 inhomogeneity effects. Using inverse Fourier transform, a suitable noise waveform is given in Fig. 2(c, d). For the intended two spectral regions, the longitudinal magnetization is randomized and therefore allowing for effective decoupling. The maximum RF amplitude in Fig. 2(c, d) is 1.42 relative to that in Fig. 1(a, b). The RF power of the new stochastic decoupling sequence ($\sum_n |rf(n)|^2$) is 51.4% of that of original pseudo noise sequence devised by Ernst (9).

A proton-decoupled localized ^{13}C MRS spectrum of the carboxylic/amide spectral region acquired from the rat brain at 11.7 Tesla is shown in Fig. 3(a). [2,5-$^{13}C_2$]glucose was infused intravenously. No. of averages = 30. Proton decoupling was achieved using Ernst's pseudo stochastic decoupling scheme. Segment length = 350 μs. At the center of the 8.5 × 6 × 8.5 mm^3 (434 μL) spectroscopy voxel,γB_2 = 498 Hz, based on separate calibrations. As shown in Fig. 3(a), signals from glutamate C5 at 182.0 ppm, glutamine C5 at 178.5 ppm, aspartate C4 at 178.3 ppm, glutamate C1 at 175.4 ppm, glutamine C1 at 174.9 ppm, aspartate C1 at 175.0 ppm, N-acetylaspartate C5 at 174.3 ppm and GABA C1 at 182.3 ppm were detected in the 173–184 ppm range. N-acetylaspartate C1 at 179.6 ppm and C4 at 179.4 ppm signals could also be seen after more signal averaging. Lipid carboxylic signals at 172.5 ppm (15) were completely suppressed by the PRESS-type spatial localization although neither outer volume suppression nor surgical retraction of the scalp under the surface coil was performed. The linewdiths of glutamate C5 and glutamine C5 in Fig. 3(a) are 7.1 and 8.3 Hz, respectively.

Fig. 3(b) shows the spectrum acquired using the proposed windowed stochastic decoupling sequence. The peak RF amplitude of the windowed stochastic decoupling sequence is 707 Hz with decoupling power ($\sum_n |rf(n)|^2$) at 51.4% of that used in Fig. 3(a). The linewdiths of glutamate C5 and glutamine C5 in Fig. 3(b) are 6.5 and 7.7 Hz, respectively. Essentially similar decoupling effect was achieved despite of the significantly reduced decoupling power deposition.

Fig. 4 compares the performance of Ernst's stochastic decoupling method with the proposed windowed stochastic decoupling method at very low decoupling power. In Fig. 4(a), the decoupling power was 12.8% of that in Fig. 3(a), corresponding to a γB_2 of 177 Hz. At this low decoupling field strength, the effect of the performance of Ernst's stochastic decoupling method is significantly degraded. The linewdiths of glutamate C5 and glutamine C5 are broadened to 11.4 and 12.6 Hz, respectively. In contrast, the windowed stochastic decoupling sequence performed reasonably well at the same low decoupling power level

(see Fig. 4(b)). There is only a relatively small increase in the linewidth of glutamate C5 (7.7 Hz, Fig 4(b)). Glutamine C5 linewidth, which is more susceptible to inadequate proton decoupling (15), increases to 10.4 Hz in Fig. 4(b). Using the windowed stochastic decoupling sequence decoupling power is restricted to the two designated spectral bands (1.91–3.90 ppm and 6.83–7.60 ppm). The actual power utilized for decoupling in Fig. 4(b) is much higher than that in Fig. 4(a) because in the latter decoupling power is evenly distributed and approximately half of the decoupling power is deposited in the 3.90–6.83 ppm region. As a result, decoupling performance at very low RF power deposition is significantly better for the windowed stochastic decoupling method.

DISCUSSION

When [2-^{13}C]glucose instead of the commonly used [1-^{13}C]glucose is infused ^{13}C labels are incorporated into glutamate and glutamine carboxylic/amide carbons while providing the same kinetic information regardless of the number of turns of the tricarboxylic acid cycle. This is because the two carbons of acetylCoA are inserted into the carbon skeleton of glutamate, glutamine and GABA with their C-C covalent bond intact (10). Unlike protons that are coupled to the commonly observed alkyl carbons, protons coupled to carboxylic/amide carbons span two clustered chemical shift regions because of the down field glutamine amide protons (In our design of the windowed decoupling sequence, the NAA aspartyl moiety H2 proton resonance at 4.39 ppm was excluded because of the very slow turnover rate of NAA (16)). To achieve low power decoupling of the carboxylic/amide carbons a decoupling sequence that can cover a broad chemical shift range while not necessarily having a large scaling factor would be required. We found that the stochastic decoupling schemes developed by Dr. Richard Ernst more than 40 years ago (9), which has been considered obsolete by the NMR community, can be used for effective decoupling at low RF power levels where cyclic coherent decoupling schemes such as WALTZ fail (10). For human brain studies performed at 3 Tesla with stochastic decoupling the time-averaged specific absorption rate (SAR) could be lowed to 0.31–0.38 W/kg (surface coil decoupling, 15) and 0.63–0.74 W/kg (volume coil decoupling, 17), both are substantially below the safety limits established by the US Food and Drug Administration and the International Electrotechnical Commission. With the advent of very high magnetic field scanners for human brain studies (e.g., 7–11.7 Tesla) proton decoupling becomes a formidable challenge even for stochastic decoupling because of the $(\gamma B_0)^2$ dependence of RF power deposition. For example, at 11.7 Tesla, the same surface coil stochastic decoupling sequence we used at 3 Tesla would lead to a SAR of ~$(11.7/3)^2$*(0.31–0.38 W/kg) = 4.7–5.8 W/kg. An approximately 50% reduction in RF power deposition would make it feasible for stochastic decoupling at 11.7 Tesla for human brain studies. The method proposed in this work therefore opens the possibility of performing stochastic decoupling experiments at very high magnetic field for human brain studies.

In addition to the Fourier method introduced here for reducing RF power deposition of in vivo stochastic decoupling other schemes for reducing RF power deposition are also conceivable. For example, one may use a sine or cosine modulation of the amplitude of a pseudo noise waveform to distribute RF power deposition over two bands of equal width. One may also use two interleaved noise sequences with different rates of linear phase increments. Both methods rely on a mixture of coherent and incoherent schemes (in comparison, the Fourier method proposed here is a pure stochastic method). For decoupling the carboxylic/amide protons, however, there is appreciable interaction between the two simultaneously applied decoupling fields due to the relatively long duration of the pulses, leading to significant degradation of decoupling performance (data not shown).

Finally, the intrinsic detection sensitivity of carboxylic/amide ^{13}C signals is less than their counterparts in the aliphatic region because their T_1s are longer as noted in the previous work (10). One key motivation for measuring ^{13}C signals in carboxylic/amide region is the exciting prospect of integrating ^{13}C MRS into the framework of parallel imaging using multiple ^{13}C receiver coils and whole-brain low power proton decoupling. Since scalp lipid signal in the carboxylic/amide region does not overlap with signals of interest it is possible to directly localize irregularly shaped cortical gray matter close to the small coils using novel localization schemes such as SPLASH (18) to achieve both sensitivity gain and high spatial specificity. The approximately 50% reduction in proton decoupling power deposition demonstrated by the current work suggest that it may be possible to study the incorporation of ^{13}C labels into metabolites in human brain at very high magnetic field strength (up to 11.7 Tesla) using windowed stochastic proton decoupling.

Acknowledgments

Contract grant sponsor: The Intramural Research Program of the NIH, NIMH.

The authors thank Dr. Jehoon Yang who participated in the initiation of this project, and Mr. Christopher Johnson for technical assistance.

References

1. Cerdan S, Künnecke B, Seelig J. Cerebral metabolism of [1,2-$^{13}C_2$]acetate as detected by in vivo and in vitro ^{13}C NMR. J Biol Chem. 1990; 265:12916–12926. [PubMed: 1973931]
2. Bottomley PA, Hardy CJ, Roemer PB, Mueller OM. Proton-decoupled, Overhauser-enhanced, spatially localized carbon-13 spectroscopy in humans. Magn Reson Med. 1989; 12:348–363. [PubMed: 2560801]
3. Chhina N, Kuestermann E, Halliday J, et al. Measurement of human tricarboxylic acid cycle rates during visual activation by (13)C magnetic resonance spectroscopy. J Neurosci Res. 2001; 66:737–746. [PubMed: 11746397]
4. Shen J, Petersen KF, Behar KL, et al. Determination of the rate of the glutamate/glutamine cycle in the human brain by in vivo ^{13}C NMR. Proc Natl Acad Sci U S A. 1999; 96:8235–8240. [PubMed: 10393978]
5. Xu S, Shen J. In vivo dynamic turnover of cerebral ^{13}C isotopomers from [U-^{13}C]glucose. J Magn Reson. 2006; 182:221–228. [PubMed: 16859940]
6. Yang J, Johnson C, Shen J. Detection of reduced GABA synthesis following inhibition of GABA transaminase using in vivo magnetic resonance signal of [(13)C]GABA C1. J Neurosci Methods. 2009; 182:236–243. [PubMed: 19540876]
7. Mason GF, Petersen KF, Lebon V, Rothman DL, Shulman GI. Increased brain monocarboxylic acid transport and utilization in type 1 diabetes. Diabetes. 2006; 55:929–934. [PubMed: 16567513]
8. Boumezbeur F, Petersen KF, Cline GW, et al. The contribution of blood lactate to brain energy metabolism in humans measured by dynamic ^{13}C nuclear magnetic resonance spectroscopy. J Neurosci. 2010; 30:13983–13991. [PubMed: 20962220]
9. Ernst RR. Nuclear magnetic double resonance with an incoherent radio-frequency field. J Chem Phys. 1966; 45:3845–3861.
10. Li S, Yang J, Shen J. Novel strategy for cerebral ^{13}C MRS using very low RF power for proton decoupling. Magn Reson Med. 2007; 57:265–271. [PubMed: 17260369]
11. Bracewell, RN. The Fourier transform and its applications. 3. McGraw Hill Publishing Company; Boston: 2000.
12. Li S, Shen J. Integrated RF probe for in vivo multinuclear spectroscopy and functional imaging of rat brain using an 11.7 Tesla 89 mm bore vertical microimager. MAGMA. 2005; 18:119–127. [PubMed: 16007474]

13. Chen Z, Li SS, Yang J, Letizia D, Shen J. Measurement and automatic correction of high-order B_0 inhomogeneity in the rat brain at 11.7 Tesla. Magn Reson Imaging. 2004; 22:835–842. [PubMed: 15234452]
14. Slotboom J, Bovée WMMJ. Adiabatic slice-selective rf pulses and a single-shot adiabatic localization pulse sequence. Concept Magn Reson. 1995; 7:193–217.
15. Li S, Zhang Y, Wang S, et al. In vivo ^{13}C magnetic resonance spectroscopy of human brain on a clinical 3 T scanner using [2-^{13}C]glucose infusion and low-power stochastic decoupling. Magn Reson Med. 2009; 62:565–573. [PubMed: 19526500]
16. Xu S, Yang J, Shen J. Measuring N-acetylaspartate synthesis in vivo using proton magnetic resonance spectroscopy. J Neurosci Methods. 2008; 172:8–12. [PubMed: 18486230]
17. Li S, Zhang Y, Wang S, et al. ^{13}C MRS of occipital and frontal lobes at 3 T using a volume coil for stochastic proton decoupling. NMR Biomed. 2010; 23:977–985. [PubMed: 20878974]
18. An L, Warach S, Shen J. Spatial localization accomplished by sensitivity heterogeneity. Proc Intl Soc Mag Reson Med. 2010; 18:25.

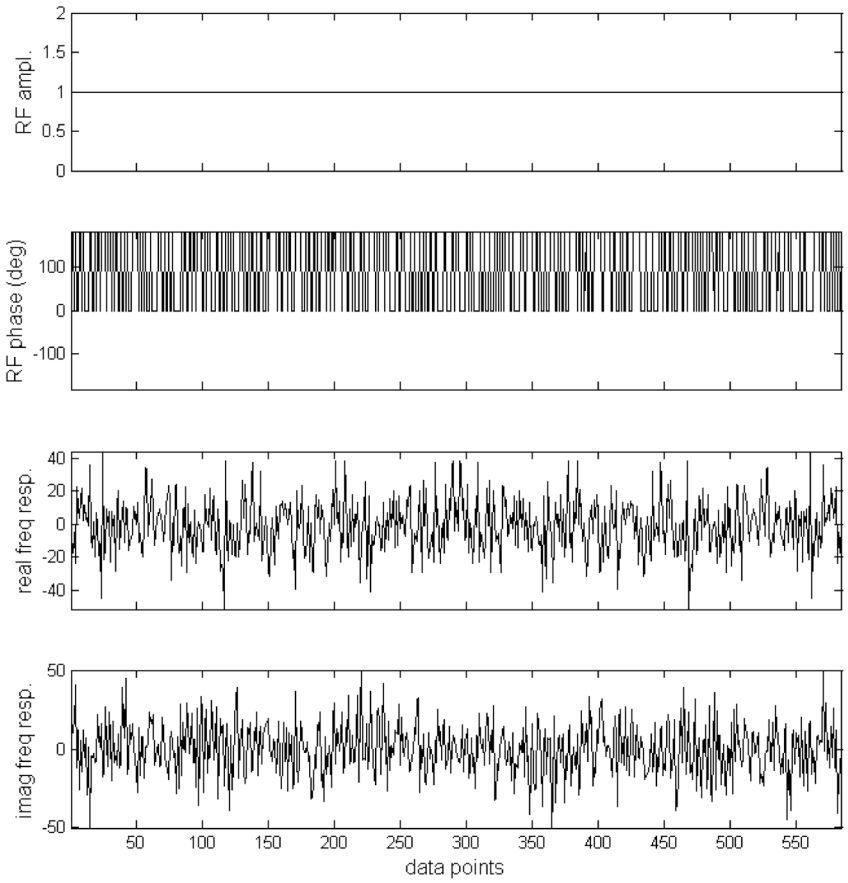

Fig. 1.

(a) Amplitude of the original pseudo stochastic decoupling sequence. (b) Phase of the original pseudo stochastic decoupling sequence by MATLAB random number generator. The phase of each segment was randomly chosen to be either 0° or 180°. A total of 585 segments were used to span the data sampling time of 204.8 ms. (c) Real component of the frequency response of the stochastic pulse depicted in (a, b). (d) Imaginary component of the frequency response of the stochastic pulse depicted in (a, b). (c, d) were generated by Fourier transformation of (a, b).

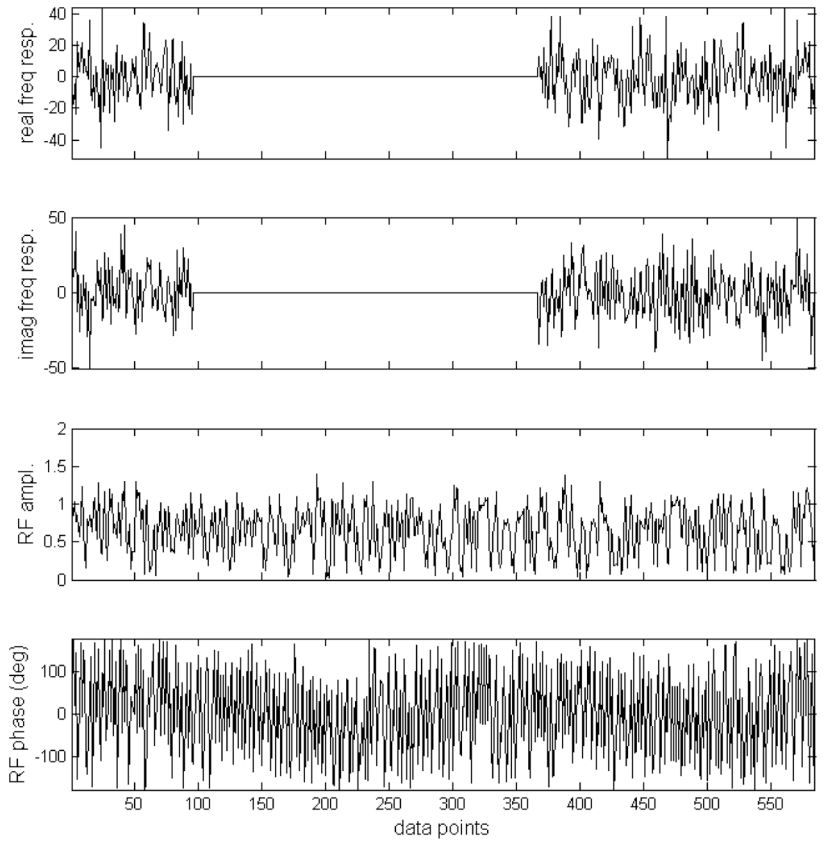

Fig. 2.

(a) The real component of the frequency response of the original pseudo stochastic decoupling sequence multiplied by an ideal double bandpass filter. The two bands correspond to the 1.91–3.90 ppm and 6.83–7.60 ppm regions with a margin of 0.1 ppm on both sides of each band. (b) The imaginary component of the frequency response of the original pseudo stochastic decoupling sequence multiplied by the same ideal double bandpass filter. (c) Amplitude of the proposed stochastic decoupling sequence generated using inverse Fourier transformation of (a, b). The maximum RF amplitude is 42% higher than that of the original pseudo stochastic decoupling sequence. The RF power of the new stochastic decoupling sequence is 51.4% of that of original pseudo noise sequence. (d) Phase of the proposed stochastic decoupling sequence.

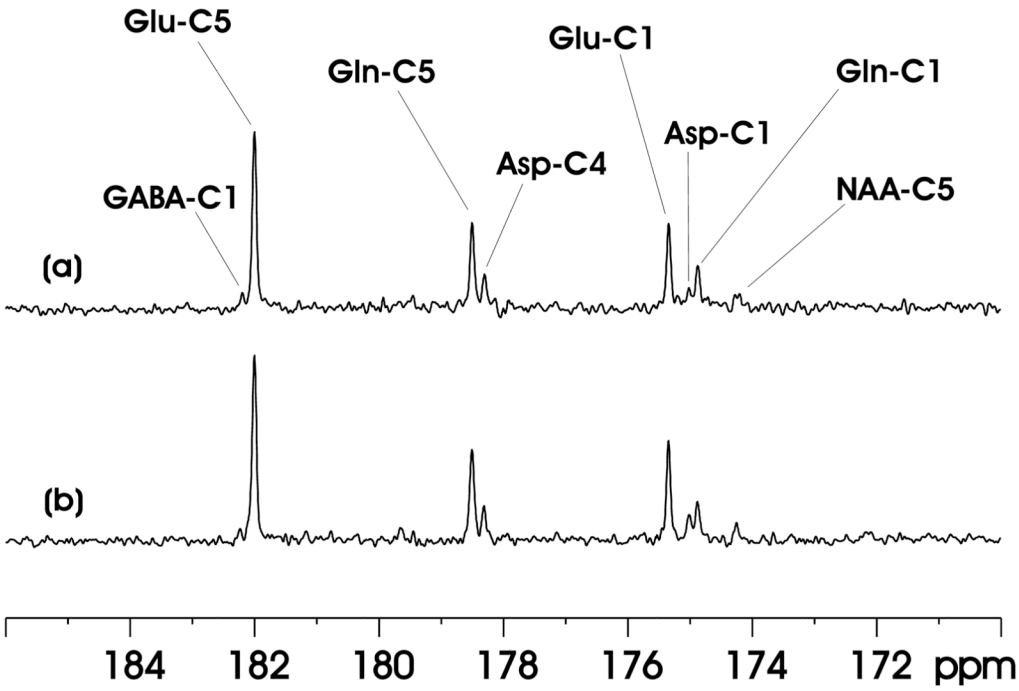

Fig. 3.

(a) A proton-decoupled localized ^{13}C MRS spectrum of the carboxylic/amide spectral region acquired from the rat brain at 11.7 Tesla during intravenous infusion of [2,5-$^{13}C_2$]glucose. Voxel size = 8.5 × 6 × 8.5 mm^3. No. of averages = 30. Ernst's pseudo stochastic decoupling scheme was used with γB_2 = 498 Hz at the center of the spectroscopy voxel. lb = −1, gb = 0.06. GABA-C1 = γ-amminobutyric acid C1, Glu-C5 = glutamate C5, Gln-C5 = glutamine C5, Asp-C4 = aspartate C4, Glu-C1 = glutamate C1, Asp-C1 = aspartate C1, Gln-C1 = glutamine C1, NAA-C5 = *N*-acetylaspartate C5. (b) In vivo ^{13}C MRS spectrum acquired using the proposed windowed stochastic decoupling sequence (Fig. 2(c, d)). The peak RF amplitude of the windowed stochastic decoupling sequence is 707 Hz with decoupling power ($\sum_n |rf(n)|^2$) at 51.4% of that used in (a). All other data acquisition and processing parameters are the same as in (a).

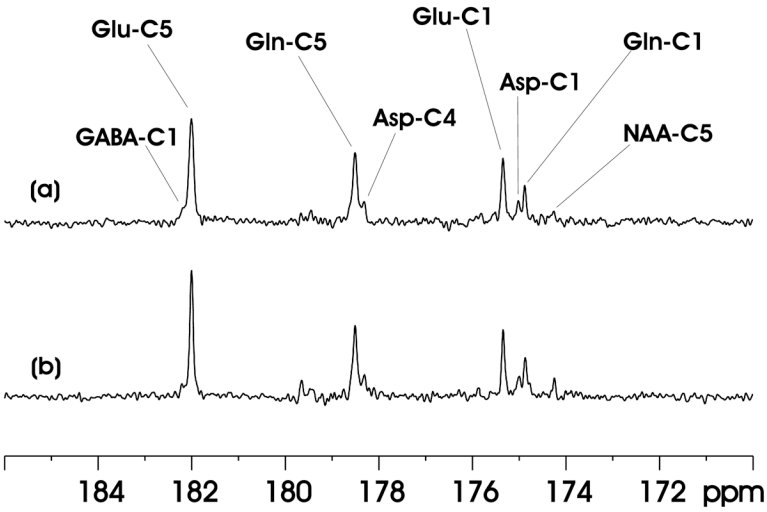

Fig. 4.

(a) In vivo ^{13}C MRS spectrum acquired using Ernst's stochastic decoupling sequence. γB_2 = 177 Hz at the center of the spectroscopy voxel. (b) In vivo ^{13}C MRS spectrum acquired using the windowed stochastic decoupling sequence shown in Fig. 2(c, d) at the same decoupling power level as in Fig. 4(a). All other data acquisition and processing parameters used in Fig. 4 are the same as in Fig. 3(a).